

## **Influence of Adding Rectangular Fins on the Performances of a Thermal Solar Air Plane Collector**

**Boukaré Ouedraogo<sup>1\*</sup>, Boureima Dianda<sup>2</sup>, Kalifa Palm<sup>2</sup>  
and Dieudonné Joseph Bahiebo<sup>1</sup>**

<sup>1</sup>*Department of Physics, Laboratory of Renewable Thermal Energies (LETRE), Faculty of Exact and Applied Sciences: UFR-SEA, University of Ouagadougou, P.O.Box: 03 - 7021 Ouagadougou 03, Burkina Faso.*

<sup>2</sup>*Department of Energy, Applied Sciences and Technologies Research Institute- IRSAT/CNRST Ouagadougou 03 BP 7047 Ouagadougou 03, Burkina Faso.*

### **Authors' contributions**

*This work was carried out in collaboration between all authors. All authors read and approved the final manuscript.*

### **Article Information**

DOI: 10.9734/BJAST/2015/20741

#### Editor(s):

(1) Abida Farooqi, Department of Environmental Sciences, Quaid-i-Azam University, Pakistan.

(2) João Miguel Dias, Habilitation in Department of Physics, CESAM, University of Aveiro, Portugal.

#### Reviewers:

(1) Anonymous, University of Missouri-St. Louis, USA.

(2) Anonymous, Dr. YS Parmar University of Horticulture & Forestry, India.

Complete Peer review History: <http://sciencedomain.org/review-history/11363>

**Original Research Article**

**Received 6<sup>th</sup> August 2015**  
**Accepted 23<sup>rd</sup> August 2015**  
**Published 12<sup>th</sup> September 2015**

### **ABSTRACT**

Low heat-air exchange in a dynamic vein of the solar collector still remains one of the major issues to solve in the use of thermal solar energy. These exchanges do not enable to achieve better performance or increased energy efficiency with these Systems. Instead, the fitting of fins on the absorber of the collector significantly improves heat transfer. So, the objective of our study is to assess the performance of a flat plate collector equipped with rectangular fins in natural and forced convections. In a theoretical study, a program to simulate the thermal performance of the transitory regime collector was established using MATLAB 7.8.0 calculation software. Regarding the experimental part, a set of measurements of solar radiation and temperatures of the fluid and the collector components were undertaken both in natural and forced convections. Theoretical and experimental results are consistent and encouraging. The maximum experimental productivity reaches 75% in forced convection and 40% in natural convection. The theoretical experimental efficiency is 84.5% in forced convection.

\*Corresponding author: E-mail: [boubakont2015@gmail.com](mailto:boubakont2015@gmail.com);

**Keywords:** Thermal collector; fin, performance; natural and forced convection.

## NOMENCLATURES

$a$	: albedo	$T$	: Air temperature in the mobile air vein of the collector ( $^{\circ}\text{C}$ )
$A$	: Collection surface of the air flat plate collector ( $\text{m}^2$ )	$T_a$	: Ambient temperature ( $^{\circ}\text{C}$ )
$DH$	: Hydraulic Diameter (m)	$T_c$	: Temperature of the vault ( $^{\circ}\text{C}$ )
$DT$	: Temperature gap ( $T_s - T_a$ ) ( $^{\circ}\text{C}$ )	$T_e$	: Air temperature at the entry of the collector ( $^{\circ}\text{C}$ )
$e_{is}$	: Thickness of the rear isolator (m);	$T_{ii}, T_{ie}$	: Temperature of the internal isolator ( $^{\circ}\text{C}$ )
$e_v$	: Thickness of the window pane (m)	$T_L^*$	: Linke air trouble factor
$F'$	: Local efficiency transfer coefficient air - absorber	$T_s$	: Air temperature at the exit of the collector ( $^{\circ}\text{C}$ )
$F_R$	: Overall transfer coefficient air – absorber	$T_{so}$	: Temperature of the floor ( $^{\circ}\text{C}$ )
$H$	: Angular height	$T_{ve}, T_{vi}$	: Temperature of the external and internal pane ( $^{\circ}\text{C}$ )
$h_{rcv}$	: Transfer coefficient by radiation between the vault and the pane ( $\text{W}/\text{m}^2\text{K}$ )	$T_n$	: Temperature of the absorber ( $^{\circ}\text{C}$ )
$h_{rmv}$	: Transfer coefficient by radiation between the pane and the absorber ( $\text{W}/\text{m}^2\text{K}$ )	$U_b$	: Thermal loss coefficient in the back of the absorber ( $\text{W}/\text{m}^2\text{K}$ )
$h_{rmi}$	: Transfer coefficient by radiation between the absorber and the isolator ( $\text{W}/\text{m}^2\text{K}$ )	$U_L$	: Thermal loss coefficient between the absorber and the ambient air ( $\text{W}/\text{m}^2\text{K}$ )
$h_{ris}$	: Transfer coefficient by radiation between the isolator and the floor ( $\text{W}/\text{m}^2\text{K}$ )	$U_t$	: Thermal loss coefficient in the front of the absorber ( $\text{W}/\text{m}^2\text{K}$ )
$h_{vv}$	: Convective transfer coefficient due to win ( $\text{W}/\text{m}^2\text{K}$ )	$V_f$	: Air speed in the mobile air vein (m/s)
$h_{vmv}$	: Transfer coefficient by natural convection between the absorber and the pane ( $\text{W}/\text{m}^2\text{K}$ )	$V_v$	: Wind speed (m/s)
$h_{vma}$	: Convective transfer coefficient between the absorber and the air ( $\text{W}/\text{m}^2\text{K}$ )	<b>Dimensionless numbers</b>	
$i$	: angle of inclination of the incident solar ray	$Re$	: Reynolds
$I_0$	: Solar constant ( $\text{W}/\text{m}^2$ )	$Nu$	: Nusselt number
$L$	: Collector length (m)	$Pr$	: Prandtl number
$l$	: Collector width (m)	<b>Greek Alphabet</b>	
$\dot{m}$	: Mass air flow (kg/s)	$\alpha_n, \alpha_v$	: Absorption coefficients of the absorber and the pane
$N$	: Number of fins	$\beta$	: Angle of inclination of the collector
$P_{\beta}$	: Overall flow received by the air flat plate collector ( $\text{W}/\text{m}^2$ )	$\varepsilon_c, \varepsilon_i, \varepsilon_v$	: Emissivities of the vault, the isolator and the pane
$P_{air}$	: Direct flow ( $\text{W}/\text{m}^2$ )	$\eta$	: Thermal efficiency of the air plan collector (%)
$P_{dif}$	: Diffuse flow ( $\text{W}/\text{m}^2$ )	$\lambda$	: Air conductivity ( $\text{W}/\text{mK}$ )
$P_{\beta}$	: Flow absorbed by the absorber ( $\text{W}/\text{m}^2$ )	$\lambda_i$	: Isolator conductivity ( $\text{W}/\text{mK}$ )
$P_u$	: Useful heat flow recovered ( $\text{W}/\text{m}^2$ )	$\lambda_b$	: Wood conductivity ( $\text{W}/\text{mK}$ )
$RG$	: Overall radiation ( $\text{W}/\text{m}^2$ )	$\nu_f$	: Air cinematic viscosity ( $\text{m}^2/\text{s}$ )
		$\nu_f$	: Air dynamic viscosity (kg/ms)
		$\sigma$	: Stephan-Boltzmann constant, ( $\text{W}/\text{m}^2\text{K}^4$ )
		$\tau_v$	: Glazing transmission coefficient

## 1. INTRODUCTION

Since its invention, solar collector still remains limited because of its low productivity in converting solar energy into thermal energy. Since then, several studies are conducted to solve this problem and turn it into a simple weakness. Then, we move from coverless collectors to window panned ones: single gazing, double glazing [1,2], combined double glazing [3] and triple glazing [4]. This has

enabled to make a major step in reducing heat loss in its exchange with the external environment. Indeed, according to H.A.M. ALI [2], the combined plastic-glass cover collector has a better optical productivity (61.40%) than a double glazing (55.20%). S. Youcef-Ali and JY Demons [5] showed in an experimental study that the triple coverage gives greater performance than double-glazed by minimizing energy losses outward. This problem is now solved. The pending issue is how to raise the low level of

heat exchange produced between the absorber and the heat transfer fluid. In this theme, several works were conducted including those by T. Letz and M. Lallemand [6] who, in their study, has showed the importance of selective absorbers for air collectors. They enable to significantly improve productivities when inflow air temperature is high.

With the view to improve the heat exchange rate transmitted to the fluid, the most commonly used possibility consists in increasing the absorber exchange surface by adding fins or heat seals. So, several types and models have been studied by researchers such as A. M. Amine [7], Aoues K. Andal [8] and M. Younes [9]. K. Aoues et al. [10] have studied both models (1 and 2) differentiated by the angle of inclination with reference to the horizontal (60 and 120°). It is clear from their work that the model-1 gives better results compared to the model-2. S. Bahria and M. Bahria Amirat [4] found that the increase in the number of heat seal rows improves the productivity of 2% when we add one row. The study by A. Ahmed al-Zaid et al. [11] enables to classify in an increasing order of efficiency and performance four different collectors as follows: collectors without heat seals (SC), transversally curved ogival heat seal collector (OCT), longitudinally curved delta heat seal collector (DCL), and lastly cross-longitudinal heat seal collector (TL).

We would like through this paper, not only to contribute to improve solar thermal collectors by studying the thermal performance of right fin collector build in the absorber, but also to see the impact of the number of fins on this performance.

## 2.2 Modelling of the Collector

Exposed to sunlight, the collector receives on its surface an overall solar flow put as follow:

$$P_{\beta} = P_{dir} + P_{dif} \quad (1)$$

$$\text{Where } P_{dif} = P_{dif,h}(1 + \cos \beta)/2 + a P_{dif,h} \frac{1 - \cos \beta}{2} (1 + \sin h) \quad (2)$$

$$\text{And } P_{dir} = I_0 C_{t-s} \exp \left[ -T_L^* \left( 0,9 + \frac{9,4}{0,89^2} \sin h \right)^{-1} \right] \times \cos i \quad (3)$$

These are the diffuse flow and the direct flow respectively. A small part of the overall flow is reflected by the pane and the great part is transmitted to the absorber, which also absorbs

$$\text{The part } P_n = (\tau_v \alpha_n) P_{\beta} \quad (4)$$

It reflects a small part on the pane like infrared rays. Since it is opaque to infrared rays, it sends them back once again toward the absorber and so on. This phenomenon is called greenhouse effect. The power absorbed  $P_n$  reduced from losses  $P_p$  is the power or useful heat flow  $P_u$  sent to the coolant:

## 2. MATERIALS AND METHODS

### 2.1 Description of the Experiment Mechanism

The solar collector we study here is designed and developed by LETRE (Laboratoire d' Energies Thermiques Renouvelables) of the University of Ouagadougou. This is an air plane collector with 3 m<sup>2</sup> collection area, or a length L = 3 m and a width l = 1 m. The collector is integrated into a drying unit.

The main components of the sensor are summarized as follows:

- Only one transparent 5 mm thick glass cover.
- A thin steel absorber plate painted in matt black which thickness is 1 mm. The height between the transparent cover and the absorber plate is 50 mm.
- The dynamic air stream of 50mm high is located between the absorption plate (black body)
- And a lower steel plate placed on the insulator.

The rear insulation is done through a polystyrene sheet of 50 mm thick and a wooden casing of 5 mm thick. Additionally, 19 straight fins are embedded perpendicularly to the absorber in the sense of the fluid flow. They are 0.8 mm thick and separated one to another of 52.63 mm.

$$P_u = A \times F_R ((\tau_v \alpha_n) P_\beta - U_L (T_s - T_a)) \quad (5)$$

$$F_R = \frac{\dot{m} \times C_p}{A \times U_L} \times \left( 1 - \exp\left(\frac{-A \cdot F' \cdot U_L}{\dot{m} \times C_p}\right) \right) \quad (6)$$

With A: the surface of the collector and  $F_R$  the overall thermal exchange efficiency of the collector.

Where the local transfer efficiency

$$F' = \frac{(U_{ar} + h_{rni}^2 + h_{vna}) h_{vna}}{(U_{av} + h_{vni} + h_{vna})(U_{ar} + h_{vna} + h_{rni}) - h_{rni}^2} \quad (7)$$

### **2.2.1 Thermal balance of the various components of the collector**

Considering that the collector is divided into a number of fictitious slides which length is  $\Delta x$  related to the coolant flow, the heat transfer equations are as follow.

#### **In the window pan**

In the external face

$$\frac{M_v C_{pv} (T_{ve}(j) - T_{ve}^*(j))}{dt} = ds \frac{P_v}{2} + h_{rv} ds (T_c - T_{ve}(j)) + h_{vv} ds (T_a - T_{ve}(j)) + h_{cv} ds (T_{vi}(j) - T_{ve}(j)) \quad (8)$$

In the internal face

$$\frac{M_v C_{pv} (T_{vi}(j) - T_{vi}^*(j))}{dt} = h_{rvn} ds (T_n(j) - T_{vi}(j)) + h_{vvn} ds (T_n(j) - T_{vi}(j)) + h_{cv} ds (T_{ve}(j) - T_{vi}(j)) + ds \frac{P_v}{2} \quad (9)$$

#### **In the absorber**

$$\frac{M_n C_{pn} (T_n(j) - T_n^*(j))}{dt} = h_{rvn} ds (T_{vi}(j) - T_n(j)) + h_{rni} ds (T_{ii}(j) - T_n(j)) + h_{vvn} ds (T_{vi}(j) - T_n(j)) + h_{vna} ds (T(j-1) - T_n(j)) + h_{vaa} \eta_1 N_{ai} ds_{ai} (T(j-1) - T_n(j)) + P_n ds \quad (10)$$

Surface of the fin for a given section

$$ds_{ai} = 2 \times e \times \Delta x \quad (11)$$

#### **In the coolant**

$$T(j) = T(j-1) + \frac{h_{van}}{m c_p} l \Delta x (T_n(j) - T(j-1)) + \frac{h_{van}}{m c_p} l \Delta x (T_{ii}(j) - T(j-1)) + \frac{h_{van}}{m c_p} \eta_1 N_{ai} 2e \Delta x (T_n(j) - T(j-1)) \quad (12)$$

$$\text{With } e \text{ the fin width } h_{van} = h_{vii} \quad (13)$$

### **2.2.2 Balance of isolator**

In the internal face

$$\frac{M_i C_{pi} (T_{ii}(j) - T_{ii}^*(j))}{dt} = h_{rni} ds (T_n(j) - T_{ii}(j)) + h_{van} ds (T(j-1) - T_{ii}(j)) + h_{ci} ds (T_{ie}(j) - T_{ii}(j)) \quad (14)$$

In the external face

$$\frac{M_i C_{pi} (T_{ie}(j) - T_{ie}^*(j))}{dt} = h_{ris} ds (T_{so} - T_{ie}(j)) + h_{vv} ds (T_a - T_{ie}(j)) + h_{ci} ds (T_{ii}(j) - T_{ie}(j)) \quad (15)$$

### **2.3 Thermal Efficiency of the Fin Collector**

This is the ratio of the power or useful flow recovered by the heat transfer fluid from the overall flow received at the surface of the collector [12].

$$\eta_{th} = \frac{P_u}{P_\beta} \quad (16)$$

By replacing  $P_u$  by its expression,  $\eta_{th}$  becomes

$$\eta_{th} = F_R \left( \tau_v \alpha_n - \frac{U_L(T_s - T_a)}{P_\beta} \right) \tag{17}$$

$$\text{Avec } P_p = U_L(T_s - T_a) \tag{18}$$

In which the overall loss coefficient is:

$$U_L = ((U_{av} + U_{ar})(2h_{rni}h_{vna} + h_{vna}^2) + 2U_{av}U_{ar}h_{vna}) / ((2h_{rni} + U_{av} + h_{vna})h_{vna}) \tag{19}$$

$$U_{av} = \left[ \frac{1}{h_{vv} + h_{rv}} + \frac{1}{h_{vvn} + h_{rvn}} \right]^{-1} \tag{20}$$

$$\text{And } U_{ar} = \left[ \frac{1}{h_{ci}} + \frac{1}{h_{cv}} \right]^{-1} \tag{21}$$

### 3. RESULTS AND DISCUSSIONS

#### 3.1 Theoretical Results

With a simulation program established in MATLAB, we have studied the influence of parameters including ambient temperature, collector length, time, flow rate of the coolant and number of fins on the fluid temperature at the exit of the collector (Figs. 1, 2, 4 and 5). Also we studied the influence of the fluid flow speed on the thermal productivity based on the DT / RG ratio (Figs. 8 and 9).

We have also compared the right fin collector with the collector without fins (Figs. 7(a) and (b)).

According to Fig. 1, the fluid temperature at the exit of the collector increases very slightly as

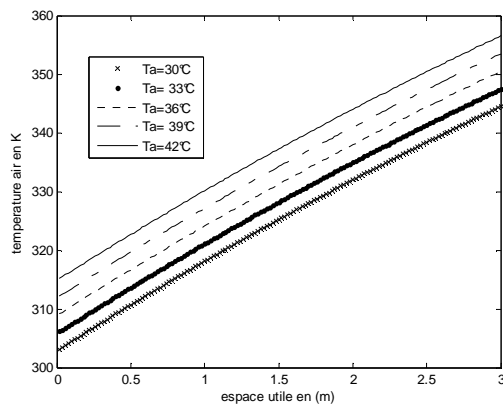


Fig. 1. Evolution of the fluid temperature according to the ambient temperature

well as the ambient temperature. The ambient temperature ( $30^\circ\text{C} \leq T_{amb} \leq 42^\circ\text{C}$ ) has little influence on that of the fluid. It can be seen in Fig. 2 that fluid temperature at the exit of the collector increases with the length according to its length. This is quite logical because the longer the collector, the longer the time the fluid will take to run through it; so it will receive more heat.

Fig. 4 shows that the temperature of the air at the exit of the drainage pipe increases with the number of fins. However, an optimum number is to be sought to efficiently ensure heat exchange. Indeed, by increasing excessively their number, the thermal inertia of the collector also increases resulting in heat losses and pressure drops. This will decrease the efficiency of the thermal collector. Over twenty (20) fins, fluid temperature variation increases slightly compared to its

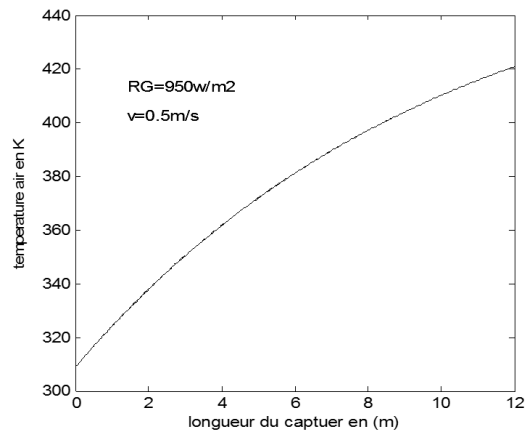
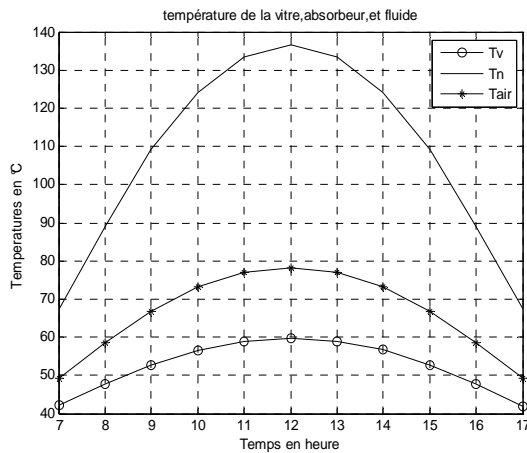
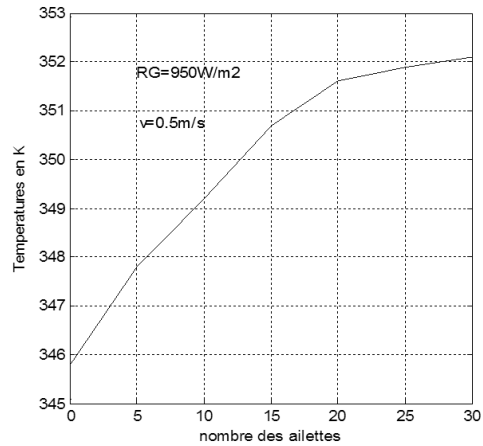


Fig. 2. Evolution of the fluid temperature according to the collector width



**Fig. 3. Variation of the temperature of the fluid, the pane and the collector**



**Fig. 4. Evolution of the fluid temperature according to the number of fins**

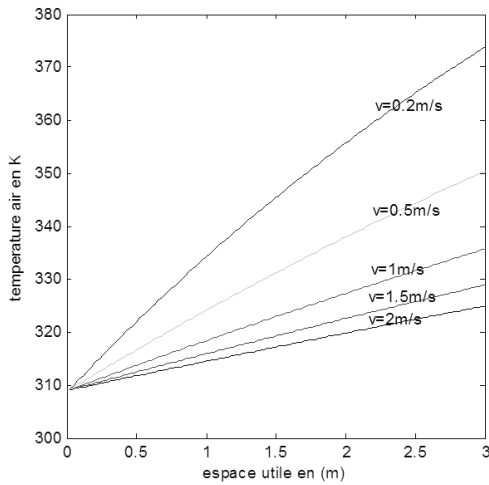


**Fig. 5. Variation of the fluid temperature according to the speed of flow**

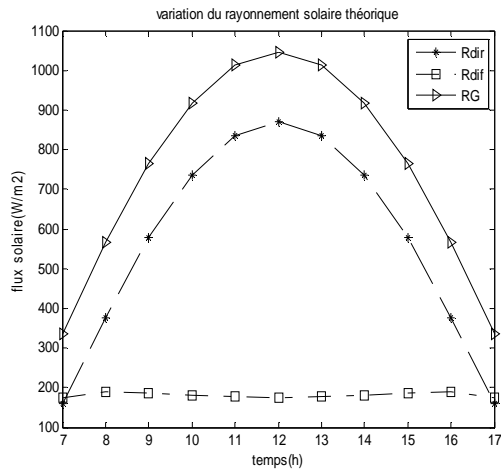


**Fig. 6. Evolution of direct ( $R_{dir}$ ), diffuse ( $R_{dif}$ ), and overall ( $R_G$ ) radiation**

below twenty (20) fins. This confirms the right choice we made to set 19 fins on the absorber. With zero fin, fluid temperature is 345.8 K while with 19 fins, it is 351.2 K, accounting for an increase of 5.4 K. we conclude that fins contribute to improve the thermal performance of the collector.

Fig. 5 shows that the speed of the fluid flow strongly impacts on the temperature at the exit of the ventilation channel. When speed increases, fluid temperature decreases. This is simply due to the fact that when the speed of the air increases, the amount of air to be heated

increases, causing temperature decrease at the exit.

When considering the Fig. 6, we notice that all these values reach their maximum at 12 h 00 min. To ensure a maximum overall radiation of  $1045 \text{ W/m}^2$  (Fig. 6), the absorber reaches  $136.55^\circ\text{C}$ , enabling therefore to raise that of the fluid to  $78.25^\circ\text{C}$  (Fig. 3). The pace of the overall radiation  $R_G$  is similar to those obtained in literature, notably by [4, 13] and by [1], with a displacement of the maximum at 13 h.

The case of the collector without fin (Fig. 7(a)) shows a positive variation of nearly  $38^\circ\text{C}$

between the temperature of the air when entering and that at the exit, against a positive variation of 58°C for the case with fins (Fig. 7 (b)), accounting for an improvement of the fluid temperature by 20°C. These results once again highlight the importance of fins on the performance of the collector. Figs. 8, 9 below show that the thermal performance of the collector increases with the flowing speed of the coolant. Yet, an exaggeration of this will contribute to decrease the performance.

### 3.2 Experimental Results

The experimental study was conducted in two parts: in natural convection and in forced convection.

#### 3.2.1 In natural convection

The results of experiments carried out with natural convection are shown in Figs. (10, 11 and 13). Natural convection is characterized by low flow velocity of the coolant. The fluid velocity is not controlled; it depends on the wind natural breath. It is therefore random. In natural convection, the thermal efficiency of the sensor is relatively low. However, the fluid temperature at the output from the flow vein of the sensor is important. This is explained by the fact that the fluid flow is slow allowing it to heat up more due to heat exchange with the absorber.

#### 3.2.2 In forced convection

The maximum fluid temperature at the exit ( $T_s$ ) is 65°C at around 12 h 15 min (Fig. 14) while the

minimum is 45°C. The interval [45° -65°C] is acceptable for a system used to dry foodstuffs like ours.

The maximum temperature at the exit in natural convection is higher (71°C) than forced convection (65°C). This is certainly due to the fact that the forced convection air volume to be heated at the same time is higher than in natural convection.

However, the maximum thermal efficiency (75%) in forced convection (Fig. 15) is considerably better than in natural convection (40%) (Fig. 12). This is due to the fact that in forced convection, the gap between the temperature at the entry and at the exit is reduced.

## 4. COMPARISON OF THEORETICAL RESULTS WITH EXPERIMENTAL

The results of the simulation and those from experiments show good similarities in form and substance. However minor differences were detected. The experimental maximum temperature of the coolant at the outlet is 70°C and is achieved between 12h30 - 12h45 (Fig. 12) is less than that of the simulation 78.25°C to 12h00 (Fig. 5). A difference of 08.25%. This can be explained by the fact that the absorber sensor was not clean enough. Indeed a fine layer of dust, but accentuated by place had deposited on the absorber during handling. Also this difference is evidently due to heat loss.

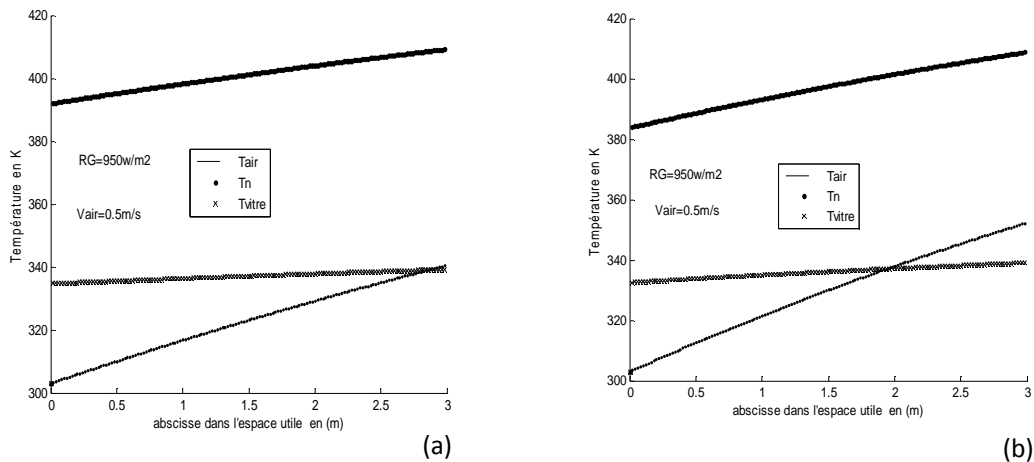
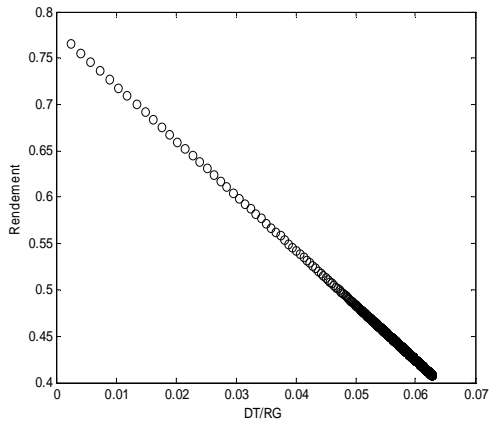
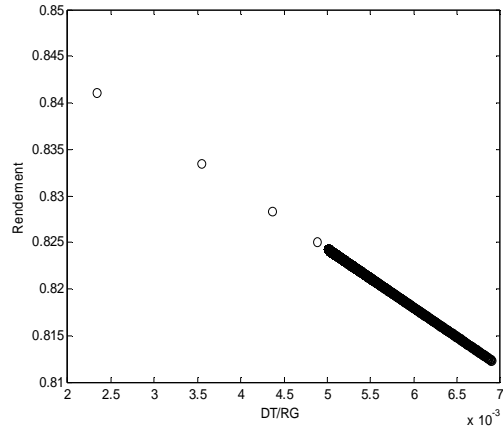


Fig. 7. Evolutions of the temperatures of the glazing, fluid, and absorber along the collector (a) without fins (b) with fins



**Fig. 8. Variation of the theoretical thermal efficiency for  $V=1.6\text{m/s}$**



**Fig. 9. Variation of the theoretical thermal efficiency for  $V=3\text{m/s}$**

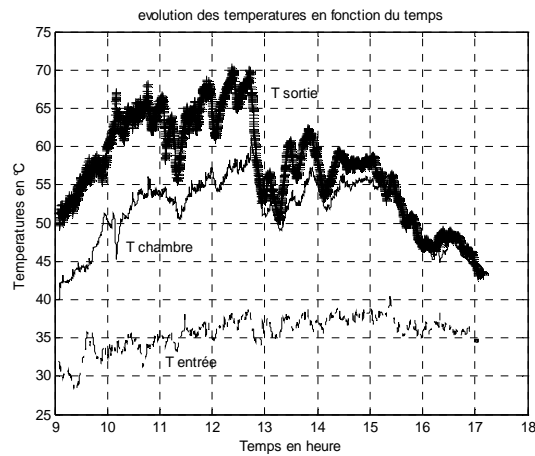


**Fig. 10. Temperature curves of the fluid at the entry, exit of the tube and in the chamber**

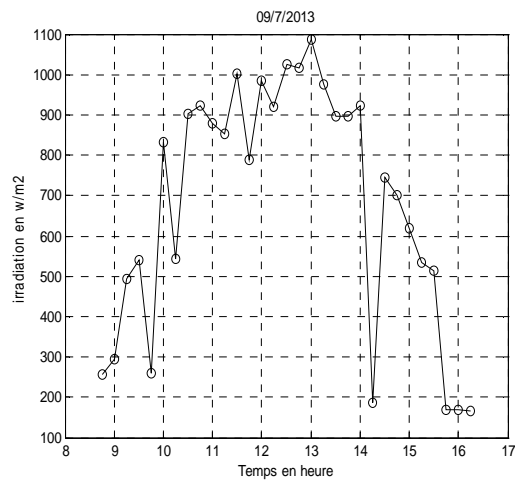


**Fig. 11. Evolution of the radiation**



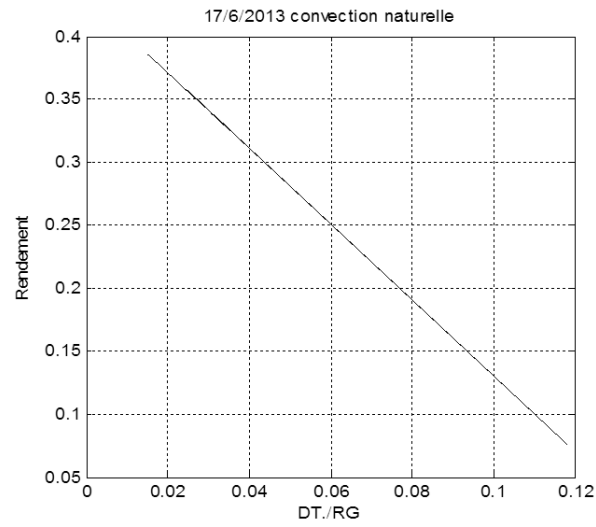


Fig. 12. Evolution of the experimental thermal efficiency in natural convection

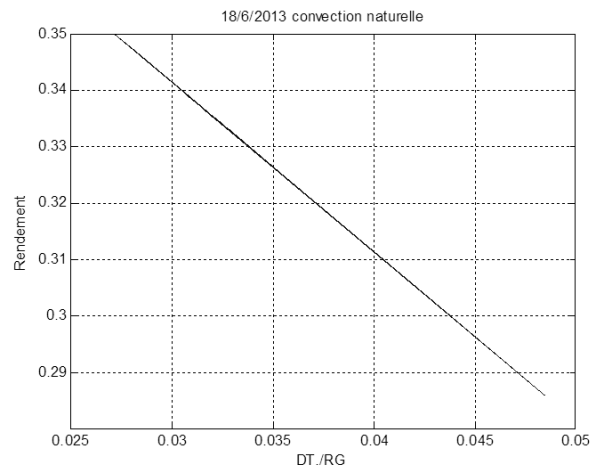


Fig. 13. Curve of the experimental thermal efficiency in natural convection

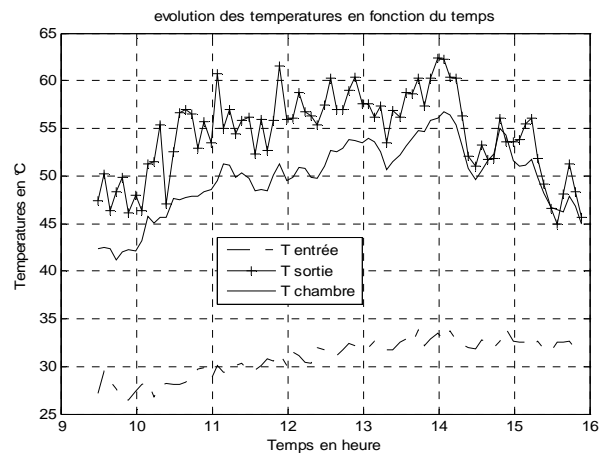
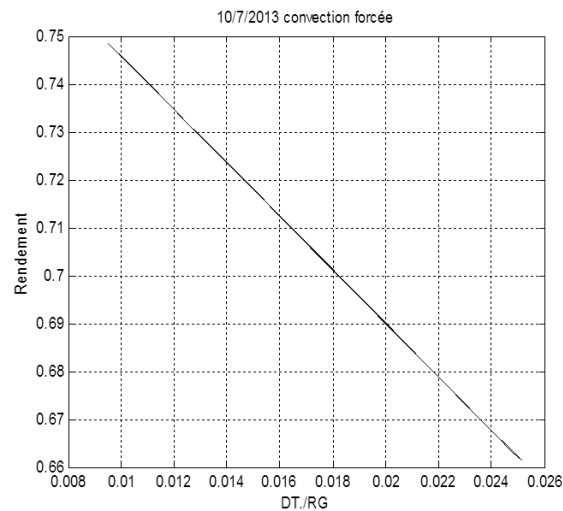


Fig. 14. Graphical representation of temperatures



**Fig. 15. Evolution of the experimental efficiency corresponding to  $v=3\text{m/s}$**

As for performance, it has to recognize that differences exist. The maximum theoretical efficiency is 84% at the velocity of 3m / s (Fig. 9) while that of the experiment is 75% at the same rate (Fig. 15). They are due precisely to the reasons that are:

- Climatic hazards: wind, clouds passing, dust in the natural.
- Heat losses in the sensor. In fact when the temperature of the absorber or the overall heat flow is uttermost, the heat loss factors which increase naturally results in an increase of heat losses as S. M. A. Bekkouche, T. Benouaz and F. Bouayad [14] have shown in their article.

As for the total radiation received at the sensor surface, the experimental values are slightly higher than theoretical. The maximum heat flow recorded during the experiments is  $1088\text{w/m}^2$  (Fig. 11) while the theoretical maximum value is  $1045\text{w/m}^2$  (Fig. 6). A difference of 3.68%. This difference is acceptable and could be explained by uncertainty about the coefficients  $a$  and  $T_L^*$  characterizing the nebulosity of the sky in the theoretical model (formulas 2 and 3).

## 5. CONCLUSION

This work was focused on the assessment of the performances of a solar thermal collector used in drying foodstuffs. In this respect, a digital model enabling to simulate the functioning of the collector, where a Computing language program "MATLAB" was developed and used. This digital

model has enabled us to study the various changes in the coolant temperature at the exit of the collector according to factors such as time, the number of fins set in the absorber, the speed of the coolant, room temperature, and the collector length. This has also enabled to study the daily thermal efficiency, and the impact of the coolant flow speed on it. The setting of a relevant number of fins (19 in our study) on the absorber improves the fluid exit temperature by  $20^\circ\text{C}$  compared to the same system operating without fins. By applying the speed 3 m / s to the coolant, we get maximal experimental and theoretical efficiencies of 75% and 84.5% respectively and maximal exit temperature of  $65^\circ\text{C}$ . We noticed that the gap between the temperature of the absorber and that of the fluid is very significant. This requires better insulation to reduce losses.

## COMPETING INTERESTS

Authors have declared that no competing interests exist.

## REFERENCES

1. Lahkdar BGM. Impact of the space between both glazings on the performance of a solar collector. Master's degree dissertation in energy physics. University Kasdi Merbah Ouargla; 2009.
2. Ali HAM. Impact of temperature gap between the absorber and the pane on the performance of the double glazing solar collector. Master's degree dissertation in

- energy physics. University Kasdi Merbahouargla; 2009.
3. Njomo D. Theoretical study of the thermal behavior of a solar air plane collector with mixed plastic-pane cover. *Thermal General Review*. 1998;37:973-980.
  4. Bahria S, Amirat M. Influence of the addition of longitudinal chicanes on the solar air plane collector performances. *Renewable Energy Review*. 2013;16(1): 51–63.
  5. Youcef-Ali S, Demons JY. Numerical and experimental study of a solar equipped with offset rectangular plate fin absorber plate. *Renewable Energy*. 2006;31:(13): 2063 – 2075.(.).
  6. Letz T, Lallemand M. Theoretical and experimental study of an solar air plane collector in a dynamic speed. *Applied Physics Review*. 1986;21 :727-734.
  7. Amine AM. 'Study of numerical solar air plane collector: influence of the form of the roughness. Master's Degree Dissertation; 2012.
  8. Aoues K, Moumami N, Moumami A, Zellouf M, Labed A, Achouri E. Study of the influence of artificial roughness on the solar air plane collectors performances. *Renewable Energy Review*. 2008;11(2): 219-227.
  9. Younes M. 'Comparative numerical study of two types of chicanes and fins (Trapezoid and Triangular) used to improve solar air plane collectors performances. Master's degree dissertation. University Abou Bekr Belkaïd Tlemcen; 2012.
  10. Aoues K, Moumami N, Zellouf M, Moumami A, Labed A, Achouri E, Benchabane A. Improving solar air plane collectors performances: Experimental study in Biskra Region. *Renewable Energy Review*. 2009;12(2):237–248.
  11. Ahmed-Zaïd A, Moulla A, Hantala MS, Desmons JY. Improving solar air plane collectors performances: Application for the drying of yellow onion and hareng. *Renewable Energy Review*. 2001;4:69-78.
  12. Dagunet M. Solar dryers, theory and practice. UNESCO, Paris (France); 1985.
  13. Taha FA. Development of a software for the simulation of solar plane thermal collector performances. Master's degree Dissertation, University Mohamed Khider-Biskra; 2013.
  14. Bekkouche, Benouaz T, Bouayad F. Thermal modeling of a solar collector water plan. 8<sup>th</sup> International Seminar on Energy Physics; 2006.

© 2015 Ouedraogo et al.; This is an Open Access article distributed under the terms of the Creative Commons Attribution License (<http://creativecommons.org/licenses/by/4.0>), which permits unrestricted use, distribution, and reproduction in any medium, provided the original work is properly cited.

*Peer-review history:*  
*The peer review history for this paper can be accessed here:*  
<http://sciencedomain.org/review-history/11363>